Exp Fluids (2011) 50:527–534
DOI 10.1007/s00348-010-0955-4

RESEARCH ARTICLE

# Power-Spectral density estimate of the Bloor-Gerrard instability in flows around circular cylinders

**M. Khor · J. Sheridan · K. Hourigan**

Received: 30 July 2008 / Revised: 25 July 2010 / Accepted: 4 August 2010 / Published online: 15 August 2010


**Abstract** There have been differences in the literature concerning the power law relationship between the Bloor-Gerrard instability frequency of the separated shear layer from the circular cylinder, the Bénard-von Kármán vortex shedding frequency and the Reynolds number. Most previous experiments have shown a significant degree of scatter in the measurement of the development of the shear layer vortices. Shear layers are known to be sensitive to external influences, which can provide a by-pass transition to saturated growth, thereby camouflaging the fastest growing linear modes. Here, the spatial amplification rates of the shear layer instabilities are calculated using power-spectral density estimates, allowing the fastest growing modes rather than necessarily the largest structures to be determined. This method is found to be robust in determining the fastest growing modes, producing results consistent with the low scatter results of previous experiments.

## 1 Introduction

The variation of the frequency of the instability waves in the shear layer separating from a circular cylinder has been studied on numerous occasions. The original observation of these shear layer instabilities was due to Bloor (1964) using hot-wire anemometry. These Bloor-Gerrard instability waves seemed to resemble the convectively unstable Kelvin–Helmholtz instability waves observed in plane mixing layers. On the basis of boundary layer theory, Bloor deduced the relationship between the frequency of the instability waves, $f_{SL}$, the Bénard-von Kármán vortex frequency, $f_{BK}$, and the Reynolds number, $Re$, to be $f_{SL}/f_{BK} \propto Re^{0.5}$, where $Re = U_\infty D/\nu$, $U_\infty$ is the free-stream velocity, $D$ is the cylinder diameter, and $\nu$ is the kinematic viscosity. Some of the subsequent studies of the instabilities include Peterka and Richardson (1969); Wei and Smith (1986); Norberg (1987); Kourta et al. (1987); Filler et al. (1991) and Prasad and Williamson (1997). In these studies, a variety of other methods, such as hot-film and video recording, were used to determine the shear layer instability frequency. More recently, the regions of both convective and absolute instabilities in cylinder wakes have been determined using hot-wire measurements by Khor et al. (2008).

In the present study, regression analyses have been undertaken on a number of the data sets published in the literature, assuming, as the previous studies did, that $f_{SL}/f_{BK}$ and $Re$ could be related by $f_{SL}/f_{BK} = ARe^B$, where $A$ and $B$ are coefficients to be determined by the regression analyses. The values of $A$ and $B$ from these analyses are presented in Table 1. It shows a range of values that the exponent $B$ could take, from 0.53 up to 0.87, indicating the large spread of results and the difficulty of determining a universal variation. The objective of these regression analyses was to investigate the differences reported in the relationship between $f_{SL}/f_{BK}$ and $Re$, in particular the correlation obtained by Kourta et al. (1987) in support of Bloor (1964), and the correlation of Wei and Smith (1986), which showed a much higher exponent. These data sets are plotted in Fig. 1; the finely spaced and low scatter data of

M. Khor · J. Sheridan (✉)
FLAIR, Department of Mechanical & Aerospace Engineering, Monash University, Melbourne, VIC 3800, Australia
e-mail: john.sheridan@eng.monash.edu.au

K. Hourigan
FLAIR, Department of Mechanical & Aerospace Engineering and Division of Biological Engineering, Monash University, Vic 3800, Australia
e-mail: kerry.hourigan@eng.monash.edu.au

**Table 1** Results of regression analyses performed on the data sets in the literature to obtain the relationship $f_{SL}/f_{BK} = ARe^B$, where $A$ and $B$ are coefficients to be determined by the regression analyses and $R^2$ is the regression correlation coefficient

| Reference | $A$ | $B$ | $R^2$ |
|---|---|---|---|
| Bloor (1964)[a] | 0.029 | 0.64 | 0.98 |
| Wei and Smith (1986)[b] | 0.005 | 0.87 | 0.95 |
| Wei and Smith (1986)[c] | 0.010 | 0.77 | 0.77 |
| Kourta et al. (1987) | 0.061 | 0.56 | 0.98 |
| Peterka and Richardson (1969) | 0.009 | 0.79 | 1.00 |
| Filler et al. (1991)[d] | 0.089 | 0.53 | 0.54 |
| Norberg (1987) | 0.035 | 0.64 | 0.99 |
| Prasad and Williamson (1997) | 0.029 | 0.65 | 0.99 |
| Norberg (1987) and Prasad and Williamson (1997) | 0.021 | 0.69 | 0.99 |

[a] Wei and Smith (1986) performed a regression analysis on three of the data points of Bloor (1964) and reported $B = 0.73$

[b] Visualisation technique data. $A$ and $B$ were reported. $R^2$ was re-calculated

[c] Hot-film anemometry data. $A$ and $B$ were reported. $R^2$ was re-calculated

[d] $A$ and $B$ were reported. $R^2$ was re-calculated

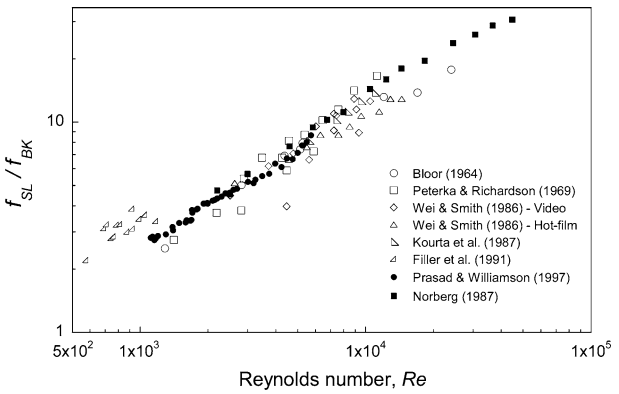


**Fig. 1** Results from past measurements of the relationship between $f_{SL}/f_{BK}$ and $Re$ from experiment without and with velocity perturbations imposed on the flow around the circular cylinder

Norberg (1987) and Prasad and Williamson (1997)) are distinguished as solid symbols. It is noteworthy that the regression analysis of the original data of Bloor (1964) yielded the value of $B = 0.64$, although Wei and Smith (1986) used three of her data points in their regression analysis to obtain $B = 0.73$. The data points from Filler et al. (1991) are quite scattered, and as a result the coefficient of correlation, $R^2$, for this set is very low.

It is also obvious from Table 1 that the regression analyses of most of the data sets yielded values of $B$ greater than 0.5. In fact, all of the data, with the exception of the data of Filler et al. (1991), appear to align better with the correlation equation suggested by Wei and Smith (1986). Regression of all the data points yielded a value of $B = 0.55$. This value would have been higher if it were not for the forced flow data set of Filler et al. (1991), which is in a lower Reynolds number range not normally associated with the appearance of shear layer vortices. In fact, Prasad and Williamson (1997) noted that despite the fact that many investigators assume the $Re^{0.5}$ dependence, their regression analysis on the data points from many of these studies resulted in an $Re^{0.69}$ dependence.

Unlike most of the other studies reported, the data of Norberg (1987) and Prasad and Williamson (1997) show little scatter and seem to have been little affected by external contamination (see Fig. 1). A re-analysis of their combined data by Thompson and Hourigan (2005) showed that indeed a *global* fit to the data produced an $Re^{0.69}$ dependence. However, importantly, the data contained *staging*; within each step, a dependence closer to the Bloor value of $Re^{0.5}$ was obtained (the exponent was slightly higher than 0.5 and explained by evolution of the boundary layer after separation). The increase in the exponent of the combined results over the individual results of Norberg (1987) and Prasad and Williamson (1997) (see Table 1) is due to the slight offset in their data (see Fig. 1), emphasising the effect of steps or offsets in regression analyses. Thus, a resolution to the long-standing problem of the correct exponent has been proposed by Thompson and Hourigan (2005), with Bloor's exponent of 0.5 approximately holding for individual steps and the higher exponent of Prasad and Williamson (1997) for global fits across steps.

The present study uses an alternative technique to measure the fastest growing modes, rather than necessarily the largest structures, in the shear layer separating from a circular cylinder, thereby circumventing the possibility of recording by-pass transitions that may arise if the flow is contaminated by background turbulence or extraneous noise. The results are then compared with the low scatter results of Prasad and Williamson (1997) and Norberg (1987).

The goals of this study were to find an experimental method that could more reliably determine the natural shear layer instability frequency, without resorting to artificially perturbing the flow or depending on the appearance of spectral peaks. This technique would then be used to determine the relationship between $f_{SL}$, $f_{BK}$ and $Re$. Furthermore, such a technique would help to affirm whether the low scatter experiments of Prasad and Williamson (1997) and Norberg (1987), commonly taken as the benchmark results for this instability, are in fact free from contaminating perturbations or systematic errors and are reproducible.

A technique to determine the spatial growth of the different instability frequencies (or modes), and therefore the peak growing frequency, is presented in Sect. 2 below, together with the details of the experimental facilities

employed in the study. The shear layer momentum thickness was measured, and the fastest growing mode frequencies for a series of experiments across a range of *Re* were determined using this spatial growth technique. These results and the relationship between $f_{SL}$, $f_{BK}$ and *Re* are presented and discussed in Sect. 3. Finally, the main findings are summarised in Sect. 4.

## 2 Experimental methods

A brief description of the wind tunnel, instrumentation and data acquisition is given below.

### 2.1 Wind tunnel

The open-circuit wind tunnel had a working section a 244 × 244 mm cross-section and a very low free-stream turbulence level: 0.07% of freestream velocity at the tunnel flow speed of 3.3 m/s. The hot-wire signal was band-pass filtered between 20 and 1,400 Hz. The flow was also highly uniform with a coefficient of variation across the whole cross-section of 0.0027. The flow velocity in the working section could be varied continuously from 1 to 35 m/s.

### 2.2 Instruments

Velocity measurements were taken with a TSI IFA-100 constant-temperature anemometer and a TSI 1210-T1.5 hot-wire probe (diameter of wire was 4 μm). The signal was processed through a Rockland 852 band-pass filter and acquired with a Boston Technology PC-30DS 12-bit ADC card mounted on an IBM PC. A pitot-static tube connected to a Van Essen 11934 Betz micro-manometer was used to take initial velocity measurements. The uncertainty of the velocity measured thus was approximately 4%. These measurements were used to calibrate the hot-wire anemometry system in the wind tunnel. The uncertainty associated with the hot-wire anemometer was estimated to be 6%.

An X-Y motorised linear traversing mechanism was constructed to traverse a hot-wire across the near wake of a circular cylinder, the hot-wire being aligned parallel to the cylinder axis. The mounting-stage was connected to a THK MTF-0601 ball-screw mechanism and controlled by a Superior Electric Slo-Syn stepping motor which stepped through 200 steps/revolution. Each step of the traverser corresponded to a movement of 5 μm to within ±0.13 microns.

The three polished Perspex cylinders used in the investigation were 244 mm long with diameters *D* of 6.29, 9.44 and 12.6 mm resulting in blockages of 2.6, 3.9 and 5.2%, respectively. Circular end-plates were mounted to reduce the influence of the boundary layer of the wind tunnel. Consequently, the effective aspect ratios of the cylinders were 32.1, 21.4 and 16.0, respectively. The co-ordinate system origin was at the centre of the cylinders midway along their length. The *x*-axis was in the direction of the flow, the *y*-axis was perpendicular to the flow, and the *z*-axis coincided with the cylinder axis.

### 2.3 Data acquisition

The main experimental programme covered the *Re* range of between 1,100 and 4,600. Depending on the size of the cylinder used, the spacing between each *y*-station was in the range 35–75 μm. The number of *y*-stations was sufficient to measure the time-mean velocity profile. Due to the symmetry of the time-mean velocity profile of circular cylinder wakes, only half the wake was traversed. Depending on the size of the cylinder used, the spacing between each *x*-station was in the range 1–2 mm. Figure 2 shows the changes that took place in the time-mean velocity profile in the near wake over a short distance, with the streamwise spacing $\Delta x/D = 0.08$.

At each sampling station, the hot-wire signal was sampled at 1,500 Hz (which was found to be sufficient for all frequencies of interest), and the sample length was 16,384. The data were then processed to calculate the mean and fluctuating velocities at each sampling station. In addition, the data were also spectrally analysed to ensure that the signals were not obviously contaminated by signal noise.

### 2.4 Calculation of the spatial growth rate of the shear layer instability using the power-spectra

Based on the assumption that the separated shear layer instability is a spatial instability and that the mean flow is nearly parallel, Soria and Wu (1992) showed that the spatial amplification rate, $\alpha_i$, of a separating shear layer

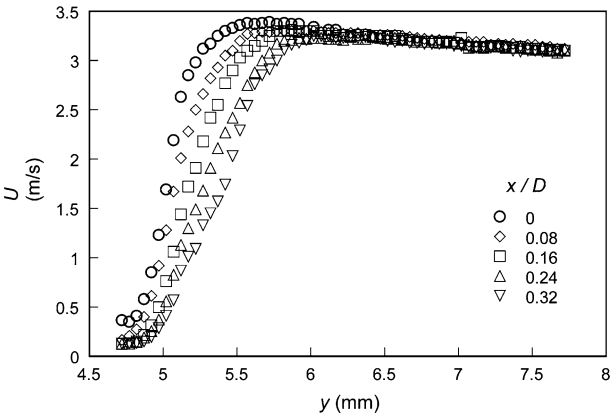


**Fig. 2** Streamwise variation in the time-mean velocity profile for five adjacent streamwise stations; $Re = 1{,}700$; $D = 9.44$ mm

instability could be calculated using the power-spectral density estimates. The spatial amplification rate varied with respect to the discrete frequency in the spectra. The $\alpha_i$ were represented as:

$$-\alpha_{i,k} = ln\frac{\hat{G}_u(x_1,f_k)}{\hat{G}_u(x_0,f_k)}/(2(x_1-x_0)), \quad (1)$$

where $\hat{G}_u$ was the power-spectral density estimate, $x$ denoted the streamwise position along the mean trajectory of the shear layer, and $k$ denoted the discrete frequency of the power-spectrum. This technique was applied by Soria and Wu (1992) to the shear layer separating from the square leading-edge of a flat plate, determining the shear layer to be convectively unstable. The effectiveness of the technique showed that the assumptions listed above were justified, even for a shear layer that had a relatively high degree of curvature. Therefore, it is expected to be suitable for the case of the circular cylinder, where the separating shear layer has a more moderate degree of curvature in the near wake.

## 3 Results and discussion

Given the desired objective of finding an experimental approach to discern the most unstable modes in the separating shear layer from a cylinder, there is a need to consider intermediate benchmarks for comparison, prior to the more global comparison against the work of Prasad and Williamson (1997) and Norberg (1987). Here, the seminal work of Michalke (1965) was chosen, as was done previously by Freymuth (1966). This comparison required that $\alpha_k$ be extracted, non-dimensionalised with the appropriate momentum thickness, $\theta$ and plotted against non-dimensional frequency, $fD/U$. The details of how this was done are discussed below.

### 3.1 Momentum thickness measurements

Detailed measurements of the velocity profiles in the near wake of the circular cylinder, made possible by the linear traverser, enabled the momentum thickness of the separated shear layers to be measured accurately. Figure 3 illustrates, with actual experimental data, the procedure followed in the calculation of the momentum thickness from the time-mean velocity profiles. The momentum thickness was calculated according to:

$$\theta = \sum_{j=1}^{M} \frac{U_j}{U_\infty}\left(1-\frac{U_j}{U_\infty}\right)\delta y, \quad (2)$$

where $U_j$ is the time-mean velocity at cross-stream station $j$, $U_\infty$ is the free-stream velocity, and $M$ denotes the station where $U_j = U_\infty$.

In the calculation, $U_\infty$ was set equal to the overshoot velocity, $U_{max}$, to avoid the negative terms that would have resulted from the overshoot in the profile. The terms calculated from $U_j < 0.5U_{max}$ were discarded because the hot-wire measurements at such low flow speeds were less accurate due to the free convection from the hot-wire. The terms calculated from cross-stream stations further out from the station where $U_j > U_{max}$ were also discarded so that there is a uniform cut-off point for every streamwise station, for every experiment run. The sum of the remaining points (denoted in Fig. 3 by the larger filled circles) was then multiplied by two to make up for the discarded $U_j < 0.5U_{max}$ terms. This was justified on the basis that, while the time-mean wake profiles of the cylinder, as fitted by the velocity profile of Monkewitz and Nguyen (1987), can be asymmetric in the far wake, for all the cases here they were found to be symmetrical about $U_j = 0.5U_{max}$. The momentum thickness of the separated shear layers grew over the $0.0 < x/D < 1.2$ range covered in the experiments. Checks were made to confirm the linearity of the growth in this region, using the non-dimensional velocity fluctuation and also the integrated kinetic energy. These techniques followed those of Unal and Rockwell (1988), and the results have been presented in detail by Khor et al. (2008). A selection of results at various $Re$ is also shown in Fig. 3. It appears that the momentum thickness growth was linear, and so regression analyses were carried out to fit straight lines through each of the momentum thickness data sets. The momentum thickness for $x/D = 0.5$ was then calculated using the resultant equation, based on this linearity and its extent.

The momentum thickness for the three cylinders is non-dimensionalised with $D$, and the variation of $\theta(x/D = 0.5)/D$ with $Re$ is shown in Fig. 4.

### 3.2 Calculation of the spatial growth rate of the shear layer instability using the power-spectra

Soria and Wu (1992) showed that the spatial amplification rate, $\alpha_i$, could be calculated using the power-spectral density estimates, for each of the discrete frequencies in the spectra. The power-spectrum of the cross-stream station with the maximum fluctuating velocity, $u'_{max}$, in the fluctuating velocity profile was used for the calculation. This ensured that there was a consistent choice of cross-stream station, the power-spectrum of which was used for the calculation, at each streamwise position. The streamwise positions, $x_0$ and $x_1$, used could be any two arbitrarily chosen positions. However, the quality of the results depended on the choice of positions, as shown below.

The results of the calculations are compared with the theoretical calculations of Michalke (1965) in his study of a two-stream mixing layer (although this was not performed

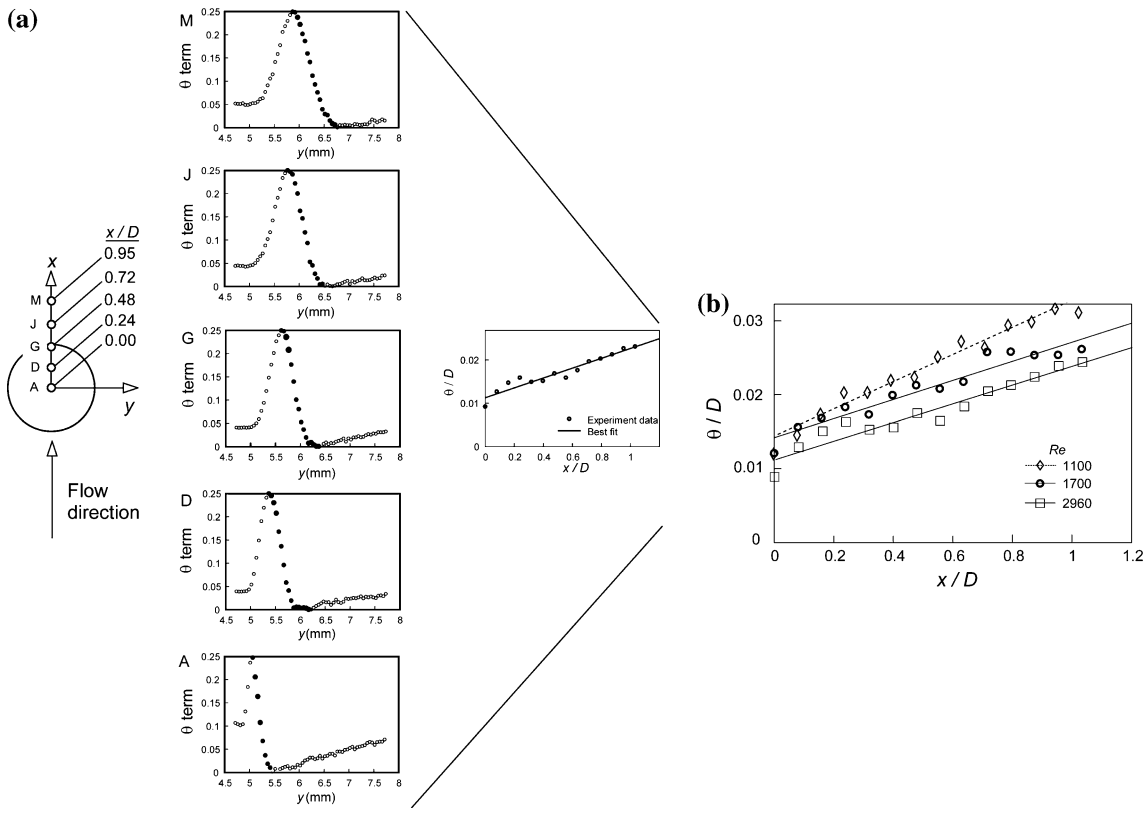


**Fig. 3** **a** Illustration of how the momentum thickness is derived for each streamwise station; $Re = 2960$; $D = 9.44$ mm. The axis label "$\theta$ term" refers to the $(U_j/U_\infty)(1 - U_j/U_\infty)$ term at cross-stream position $j$. The results from each streamwise position are combined into a graph of the streamwise variation of the momentum thickness. **b** Streamwise variation of the momentum thickness with the regression analysis lines for $Re = 1{,}100$, 1,700 and 2,960

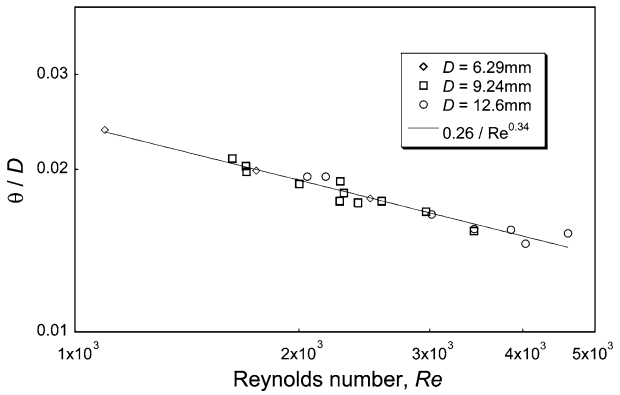


**Fig. 4** The normalised momentum thickness, $\theta/D$, at $x/D = 0.5$. The power law line of best fit is also plotted for comparison

by Soria and Wu (1992) due to insufficient flow information). The convention used by Michalke (1965) was to non-dimensionalise the $\alpha_i$ by multiplying it with the momentum thickness in the middle of the exponential growth region $\theta_m$:$\alpha_i\theta_m$. The frequency was non-dimensionalised with $\theta_m$ and the velocity of the high-speed stream of the mixing layer $U_1$, i.e., $f\theta_m/U_1$. For this section of the present study, $\theta_m$ is approximated by $\theta(x/D = 0.5)$ which is calculated using the regression equation derived from the measurements in the above section, and $U_1$ is approximated by $U_\infty$.

Comparison between the growth rates for different pairs $(x_0,x_1)$ of the streamwise positions for $Re = 1{,}100$, varying $x_0/D$ and keeping $x_1/D = 0.96$, is shown in Fig. 5. Comparison between the growth rates for different pairs $(x_0,x_1)$ of the streamwise positions for $Re = 1{,}100$, varying $x_1/D$ and keeping $x_0/D = 0.32$ is shown in Fig. 6. Also shown in each plot is the curve from the theoretical calculations by Michalke (1965).

It is clear that the larger streamwise spacings, $x_1 - x_0$, tend to produce plots that show smaller scatter between the data points and better agreement with the theoretical calculations. Also, it is seen to be preferable to choose the initial streamwise position to be sufficiently far downstream of the point of separation of the boundary layer. As would be expected, it appears that the streamwise spacing had to be sufficiently large for the growth rate of the disturbance at different frequency bands to be distinguishable from the background noise and that the structures produce stronger signals as they develop downstream. However, importantly, it is noted that the position of peak growth rate is not too sensitive to the precise value of the pair $(x_0,x_1)$;

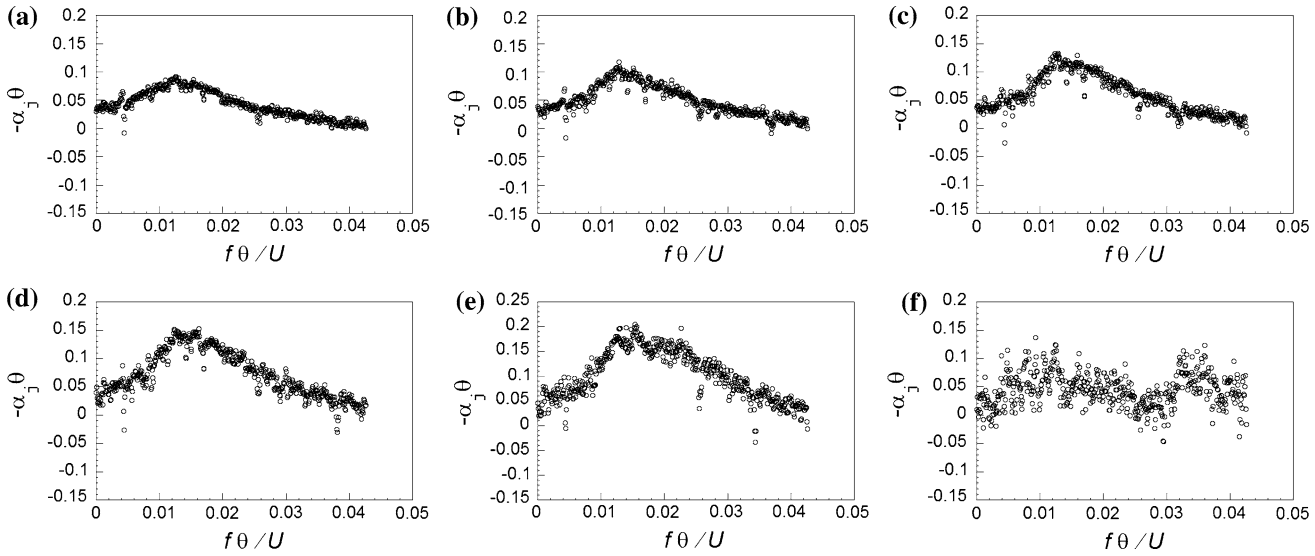


**Fig. 5** Calculations of the $\alpha_i$ using the power-spectra of the velocity time-series in the separated shear layers from the cylinder for $x_1/D = 0.96$ and different values of $x_0/D$: **a** $x_0/D = 0.00$; **b** $x_0/D = 0.16$; (**c**) $x_0/D = 0.32$; **d** $x_0/D = 0.48$; **e** $x_0/D = 0.64$; and **f** $x_0 = 0.80$. $Re = 1{,}100$ and $D = 6.29$ mm

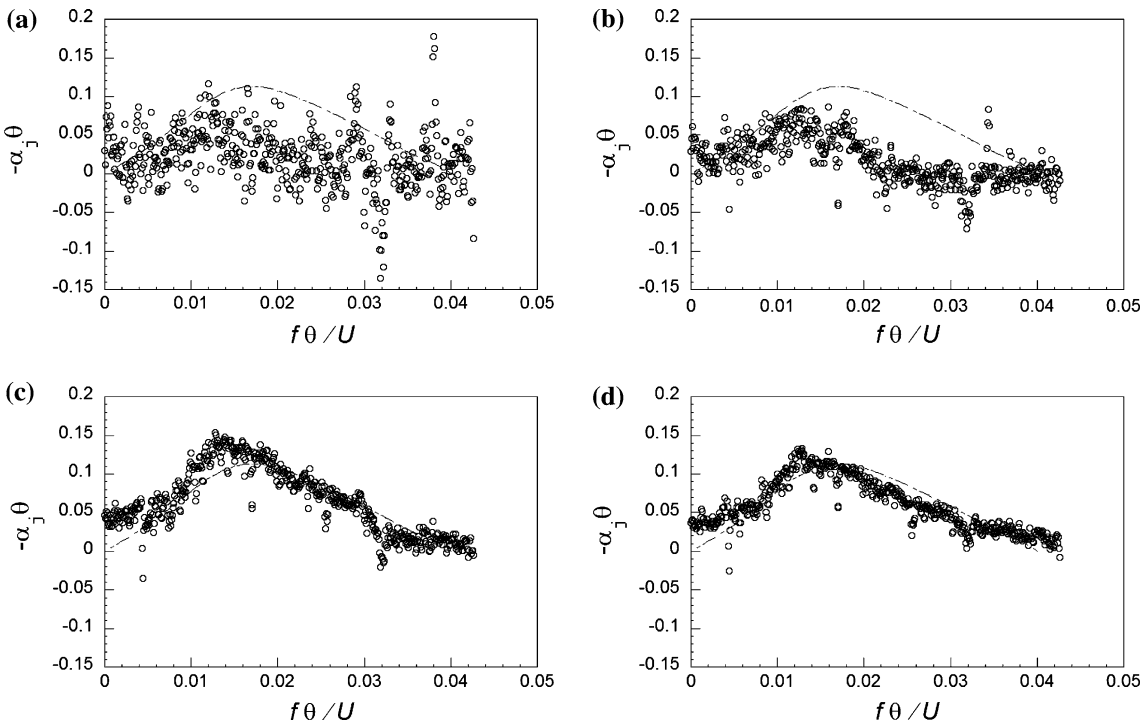


**Fig. 6** Calculations of the $\alpha_i$ using the power-spectra of the velocity time-series in the separated shear layers from the cylinder for $x_0/D = 0.32$ and different values of $x_1/D$: **a** $x_1/D = 0.48$; **b** $x_1/D = 0.64$; **c** $x_1/D = 0.80$; and **d** $x_1/D = 0.96$. $Re = 1{,}100$ and $D = 6.29$ mm. Also shown in *each plot* is the curve from the theoretical calculations of Michalke (1965)

for example, the frequencies at the peaks for $Re = 1{,}100$ in Fig. 5c–e are found to be within 5%.

Figure 7 presents plots of the growth rate curves with relatively lower scatter for a range of Reynolds numbers. Clearly seen are the peaks in the growth rates. The frequency of the fastest growing shear layer instability was determined from the calculations of the $\alpha_i$ by determining the frequency at the peak in the plots of the $\alpha_i$ at each $Re$ (using a 9th order polynomial regression to find the local peak). Uncertainty in the frequencies was due mainly to the broadness of the peaks in the spatial growth rate plots and some degree of scatter of data points. The results are

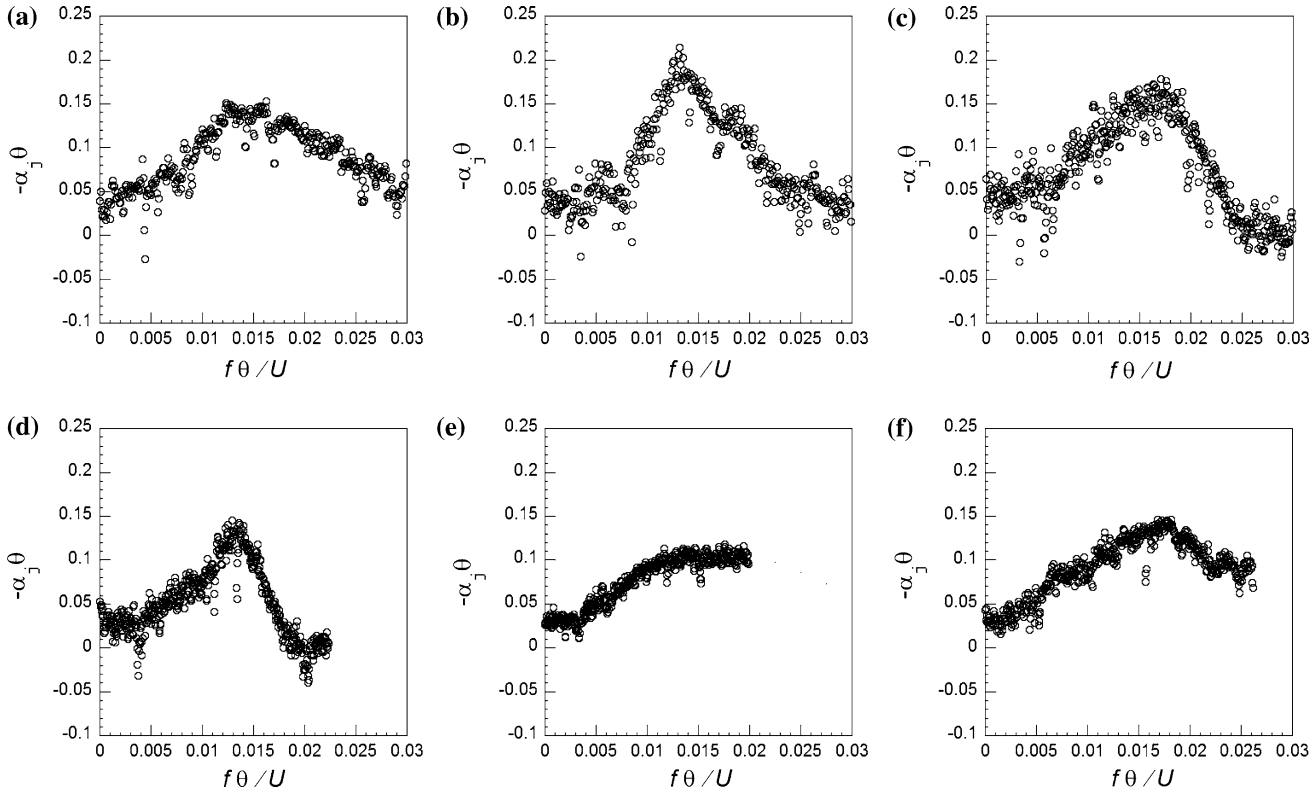


**Fig. 7** Calculations of the $\alpha_i$ using the power-spectra of the velocity time-series in the separated shear layers from the cylinder for different Reynolds numbers: **a** $Re = 1{,}100$, $D = 6.29$ mm; **b** $Re = 2{,}000$, $D = 9.44$ mm; **c** $Re = 2{,}300$, $D = 9.44$ mm; **d** $Re = 2{,}960$, $D = 9.44$ mm; **e** $Re = 3{,}440$, $D = 12.6$ mm; and **f** $Re = 4{,}600$, $D = 12.6$ mm

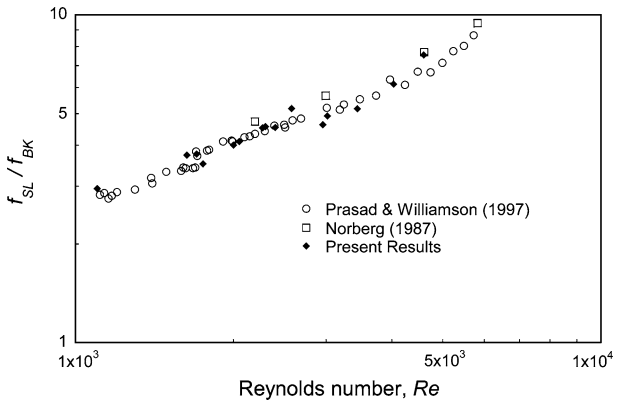


**Fig. 8** The results of the fastest growing shear layer instabilities from the $\alpha_i$ calculations together with the results of Prasad and Williamson (1997) and Norberg (1987) (the data were derived using $x_0 = 0.48$ and $x_1 = 0.96$)

presented in Fig. 8 together with the results of Prasad and Williamson (1997) and Norberg (1987). Although there is some scatter, the results of the present experiments are seen to match well with these previous results.

The results are also consistent with the staged fit to the frequency ratio vs Reynolds number proposed by Thompson and Hourigan (2005), augmenting the global fit determined by Prasad and Williamson (1997). In this case, it appears that mostly the overlap is in the lower of the two fits seen there, but the highest Reynolds number point appears to match up with the results of Norberg (1987) at higher *Re*.

Clearly, the results presented here further confirm the quality of the two low scatter data sets of Prasad and Williamson (1997) and Norberg (1987), discussed above, and their adoption as the benchmark for this particular flow. The importance of this lies in the different approach taken here in extracting the frequencies of the fastest growing instability modes and avoiding modes due to external forcing. These data appear to be subject to neither systematic nor random errors.

The other important feature of these results is that the data used here when analysed using other techniques provided more scattered results. Using this method can extract underlying growth mechanisms; however, as evidenced by the results of Prasad and Williamson (1997) and Norberg (1987) there remains no substitute for quality data.

## 4 Conclusions

Determining the shear layer instability frequency by inspecting the power-spectral plot for peaks can be prone to

spurious peaks caused by contamination of the fluid flow in the experimental facility. The method of calculating the spatial growth rate of the shear layer instability using the power-spectra, suggested by Soria and Wu (1992), provides a way of determining the shear layer most amplified instability frequency without resorting to global excitation of the flow and avoids the misleading peaks in the power-spectral plots due to flow contamination.

The most unstable frequencies in the shear layer in the near wake of a circular cylinder were determined using this technique. These were then analysed to elicit the underlying $f_{SL}/f_{BK} - Re$ relationship. It emerged that the $f_{SL}/f_{BK} - Re$ relationship obtained in the current study matches well with the previously published low scatter results of Prasad and Williamson (1997) and Norberg (1987).

**Acknowledgments** We are greatly indebted to Martin Welsh for providing the experimental facilities at the CSIRO. Moses Khor acknowledges the support of a Monash Graduate Scholarship. This research was supported under Australian Research Council's Large Grant Projects funding scheme A89131241.

## References

Bloor M (1964) The transition to turbulence in the wake of a circular cylinder. J Fluid Mech 19:290–304

Filler J, Marston P, Mih W (1991) Response of the shear layers separating for a circular cylinder to small amplitude rotational oscillations. J Fluid Mech 231:481–499

Freymuth P (1966) On transition in a separated boundary layer. J Fluid Mech 25:683–704

Khor M, Sheridan J, Thompson MC, Hourigan K (2008) Global frequency selection in the observed time-mean wakes of circular cylinders. J Fluid Mech 601:425–441

Kourta A, Boisson H, Chassaing P, Ha Minh H (1987) Nonlinear interaction and the transition to turbulence in the wake of a circular cylinder. J Fluid Mech 181:141

Michalke A (1965) On spatially growing disturbance in an inviscid shear layer. J Fluid Mech 23:521–544

Monkewitz PA, Nguyen LN (1987) Absolute instability in the near-wake of two-dimensional bluff bodies. J Fluids Struct 1:165-184

Norberg C (1987) Effects of Reynolds number and a low-intensity freestream turbulence on the flow around a circular cylinder. PhD thesis, Chalmers Univ Technol Publ No 87/2, S-412-96. Goteborg, Sweden

Peterka JA, Richardson PD (1969) Effects of sound on separated flows. J Fluid Mech 37:265–287

Prasad A, Williamson C (1997) The instability of the shear layer separating from a bluff body. J Fluid Mech 434:235–265

Soria J, Wu J (1992) The character of the instability of the separated shear layer from a square leading edge flat plate. In: Davis MR, Walker GJ (eds) Proceedings of 11th Australasian fluid mechanics conference, 14–18 Dec., Hobart, Australia, pp 391–394

Thompson MC, Hourigan K (2005) The shear layer instability of a circular cylinder wake. Phys Fluids 17:021702–021705

Unal MF, Rockwell D (1988) On vortex shedding from a cylinder Part 1. The initial instability. J Fluid Mech 190:491–512

Wei T, Smith CR (1986) Secondary vortices in the wake of circular cylinders. J Fluid Mech 169:513